4

Tidal Residual Currents and Sediment Transport Through Multiple Tidal Inlets

James T. Liu and David G. Aubrey

Abstract

Tidal residual currents in a tidal channel connecting two water bodies having contrasting tides are most sensitive to the mean sea-level differences, less sensitive to the tidal amplitude differences, and least sensitive to the tidal phase differences between the two ends of the channel. On the other hand, tidal phase difference is the most important factor in generating M_4 overtide in the channel, the tidal amplitude difference has intermediate impact on M_4 generation, and the mean sea-level difference has little effect on M_4 generation. Residual currents and M_4 overtide are generated by different mechanisms. The former is related to the friction in the system, and the latter is related to the kinematic non-linearity in the system. The combined influence of the tidal phase, amplitude, and mean sea-level differences on the generation of tidal residual currents in a channel is complex and non-linear, and can be predicted properly only by non-linear numerical models. The sediment transport patterns in a tidal channel that connects two bodies of water having different tidal characteristics can be attributed to residual currents that is primarily caused by the mean sea-level difference, and to a minor degree, by the tidal amplitude and phase differences between the two ends of the channel. Multiple inlets at Chatham, Massachusetts, are used as a case study.

Formation and Evolution of Multiple Tidal Inlets
Coastal and Estuarine Studies, Volume 44, Pages 113-157

Introduction

The tidal-mean exchange of salt, pollutants, suspended material, and sediments through a coastal channel respond to residual currents. In weakly-to-strongly non-linear estuaries, bays, and channels, the dominant tide is the primary generator of residual currents (Cotter, 1974; Tee, 1976, 1977; van de Kreeke, 1978, 1980; Ianniello, 1977, 1979; Huang et al., 1986; Wong, 1989).

Tidally generated residual currents in a channel have been shown to be influenced by the tidal amplitude, phase, and mean sea-level differences between the two open boundaries (van de Kreeke, 1980; Huang et al., 1986; Wong, 1989), and by the geometric asymmetry of the channel between the two open ends (Cotter, 1974). The present study further investigates the individual importance of the dominant tidal amplitude, phase, and mean sea-level difference on the tidal characteristics and the generation of residual currents in the interior of an open channel through diagnostic numerical modeling exercises. The model findings are then used to interpret field observations from a tidal channel that connects two bodies of water having different tidal characteristics. The effect of the residual currents on the long-term sediment transport in that channel is deduced from historical evidence.

Study Site

Chatham Harbor is a bar-built, multiple-inlet system located at the southeastern corner of Cape Cod, Massachusetts (Fig. 1). The barrier spit (Nauset Beach) that separates the estuary from the Atlantic Ocean had been accreting southward since the late 1800's until January, 1987, when it was breached during a severe storm to form a new tidal inlet (Giese, 1988). West Channel (a tidal inlet), the focus of this study, separates Monomoy Island from Morris Island, linking Nantucket Sound indirectly with the Atlantic Ocean through the southern part of the estuary (Fig. 1).

West Channel was formed in 1957 when Monomoy Island detached from Morris Island. From the early 1960's to the early 1970's before the southern tip of Nauset Beach overlapped with Monomoy Island, West Channel was directly under the influence of the coastal waves and longshore currents of the

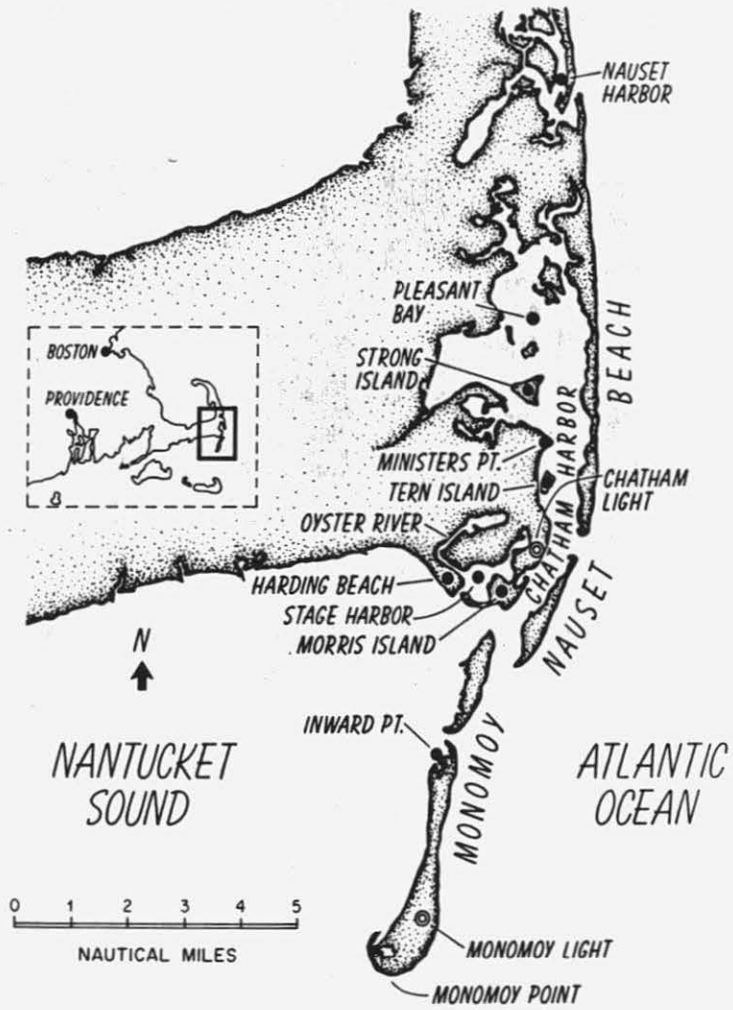

Figure 1. Index map for Chatham Harbor, Massachusetts.

Atlantic Ocean. Documentation of sand bodies and associated bedforms on either side of West Channel and measurements of tidal currents on the Nantucket side of the inlet in the early 1970's (Hine, 1975) suggested a dominant sediment transport from the Atlantic Ocean into Nantucket Sound. About 1975, Nauset Beach extended south of West Channel, gradually sheltering this inlet from the direct impact of Atlantic Ocean waves.

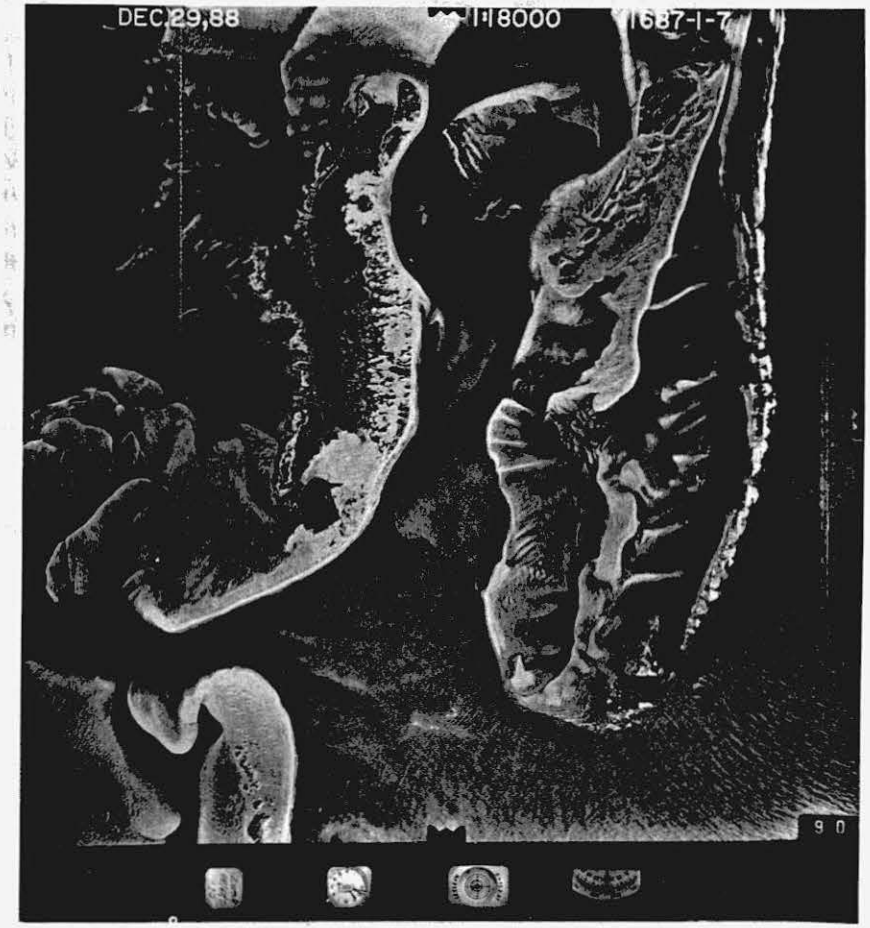

Figure 2. Vertical aerial photograph of the breach on Monomoy Island (lower left corner) taken in December, 1988. The Atlantic Ocean is on the right hand side of the breach, and Nantucket Sound is on the left.

In 1978, Monomoy Island was breached approximately 3.6 km south of West Channel (Fig. 2). Since then, extensive sand bodies have enlarged on the Nantucket side of the breach, resembling a flood tidal delta-complex consisting of superimposing spillover lobes. Little sand has accumulated on the Atlantic side of the breach (Fig. 2). This imbalance of sediment deposition between the two sides of the breach suggests a net sediment transport from the Atlantic Ocean to Nantucket Sound (Liu et al., 1989), though greater longshore sand transport on the Atlantic side undoubtedly plays some role.

Recent aerial photographs taken between May and December, 1988, document shoal development and sand flat growth on the Nantucket side of West Channel, indicating a dominant westward sediment transport following the recent breach of Nauset Beach (Liu et al., 1989). Because of the consistency in sediment transport dominance observed in West Channel and the breach on Monomoy Island, we hypothesize that tidal elevation differences between Nantucket Sound and the Atlantic Ocean generate residual flows controlling sediment transport.

In April, 1988, two digitally-recording tide gauges were deployed for 29 days in the southern part of Chatham Harbor: one due east of West Channel, and one in Nantucket Sound near the western end of the inlet (Fig. 3). During the same period, a shorter (7-day) record of near-bed current speed and sea-surface height was obtained from the middle of West Channel approximately 750 m from the tide gauge in south Chatham Harbor, and 1250 m from the tide gauge in Nantucket Sound (Fig. 3). Prior to deployment, the electromagnetic current meter was calibrated in the laboratory to yield expected mean errors of 1 to 2 cm/sec. The bathymetry in south Chatham Harbor and West Channel was surveyed using an integrated navigation system.

Thirty-five tidal constituents were resolved for each of the two tidal records (Fig. 4; the major constituents are listed in Tables 1 and 2). The M_2 tide is the largest tide in both south Chatham Harbor and Nantucket Sound. The tidal amplitude in south Chatham Harbor is 40 cm greater than that in Nantucket Sound. The M_2 phase in Nantucket Sound leads that in south Chatham Harbor by 5.5 degrees (Tables 1 and 2).

Tidal currents in the middle of West Channel show strong westward (positive) flows having a maximum speed of approximately 120 cm/sec, which is about

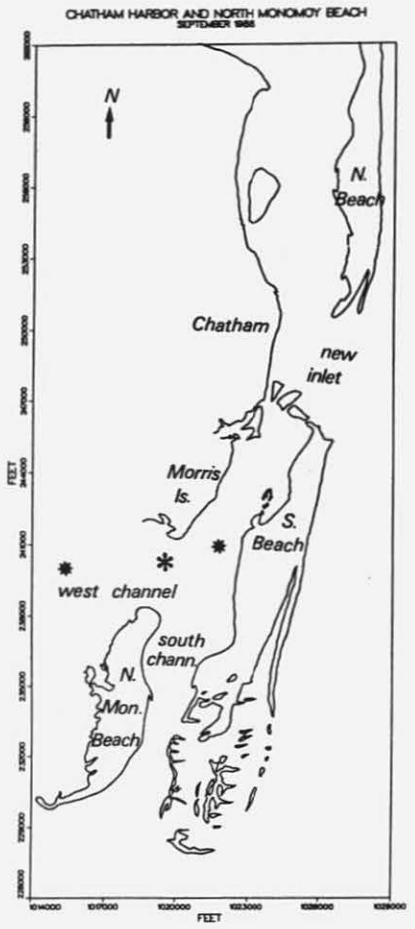

Figure 3. Detailed map showing the study area. The two asterisks represent locations of the two tide gauges deployed in south Chatham Harbor and Nantucket Sound. The middle symbol marks the location of the current meter deployment.

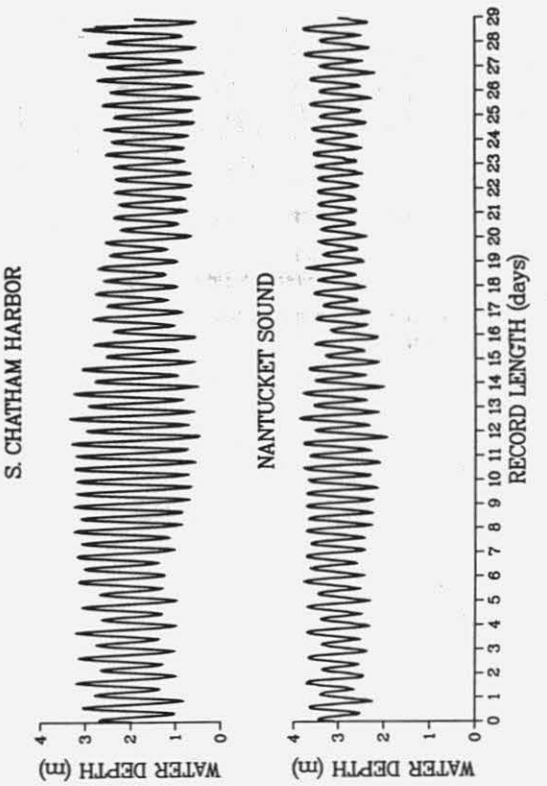

Figure 4. Tidal height records from south Chatham Harbor and Nantucket Sound.

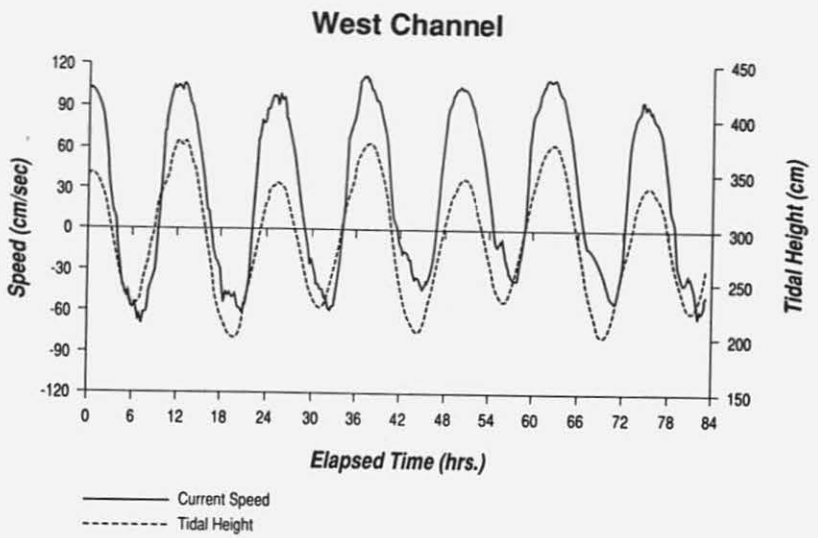

Figure 5. Instantaneous current speed (solid line) and sea-surface (dashed line) record from West

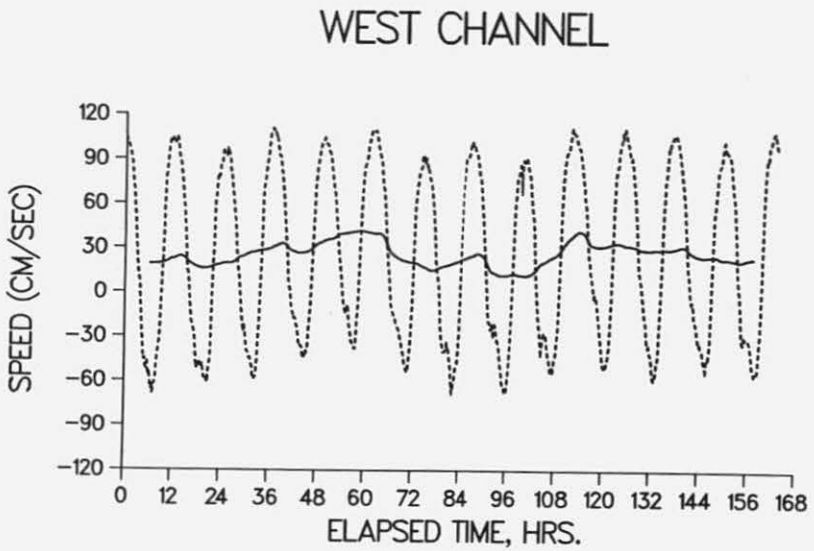

Figure 6. Instantaneous tidal current speed (dashed line) and tidally averaged residual current (solid line) in West Channel.

TABLE 1. Major Tidal Constituents in south Chatham Harbor.

Constituent	Period (hr.)	Amplitude (m)	Greenwich Phase (degrees)	% Total Energy
M_2	12.42	0.97	99.5	87.53
S_2	12.0	0.17	123.4	2.91
N_2	12.66	0.187	50.5	3.27
K_1	23.93	0.133	191.9	2.20
M_4	6.21	0.03	104.8	0.08
RMS Tidal Height = 1.98 m				

TABLE 2. Major Tidal Constituents in Nantucket Sound.

Constituent	Period (hr.)	Amplitude (m)	Greenwich Phase (degrees)	% Total Energy
M_2	12.42	0.561	94.0	82.54
S_2	12.0	0.091	119.0	2.33
N_2	12.66	0.136	43.8	4.89
K_1	23.93	0.099	175.5	3.43
M_4	6.21	0.048	296.1	0.57
RMS Tidal Height = 1.18 m				

twice the maximum of the eastward flows (Fig. 5). The phase equality between tidal current speed and sea-surface elevation suggests a progressive tide propagating through the inlet. To examine the residual velocity, the current speed record was averaged over the M_2 period (12.42 hr.) yielding a flow from south Chatham Harbor into Nantucket Sound (Fig. 6). This residual current displays some subtidal variation, about a mean speed of 26 cm/sec to the west.

Field data document flow in West Channel from greater tidal amplitude (south Chatham Harbor) to smaller tidal amplitude (Nantucket Sound). However, the contributions to residual flow from the tidal phase difference and mean sea-level difference (of which we have no direct observations) are unclear. Therefore, modeling was used to investigate the relative influences of tidal amplitude, phase, and mean sea-level difference on the generation of residual currents in a hypothetical channel to determine the relative importance of the three factors. The findings are then related to the field observations from West Channel.

Definitions and Model Formulation

The vertically averaged transport ($\bar{q}$) in a tidal channel is defined as:

$$\bar{q} = \bar{u}\,(h+\eta) \tag{1}$$

in which $\bar{u}$ (t) is the vertically averaged instantaneous Eulerian velocity, h is the still water depth, and η (t) is the sea-surface elevation. The time average over the M_2 period yields the residual flow:

$$\langle\bar{q}\rangle = \langle\bar{u}h\rangle + \langle\bar{u}\eta\rangle = \langle\bar{u}\rangle\, h + \langle\bar{u}\eta\rangle \tag{2}$$

The first term on the right hand side of equation 2 is directly proportional to the Eulerian mean flow:

$$U_E = \langle\bar{u}\rangle \tag{3}$$

The second term, the Stokes transport (assuming small amplitude long waves), results from the co-oscillation of the sea-surface elevation and the instantaneous velocity, $\bar{u}$. The Stokes drift is obtained by depth-averaging

the second term on the right hand side of eq. 2:

$$U_S = \frac{\langle\bar{u}\eta\rangle}{h} \tag{4}$$

The depth-averaged Lagrangian velocity U_L is:

$$U_L = U_E + U_S \tag{5}$$

A straight east-west oriented (x-axis positive towards the west) channel, 2 km in length (Fig. 7), having a constant trapezoidal cross-section with tidal flats on both sides, is used to represent West Channel (Fig. 8).

The governing equations for the one-dimensional, cross-sectionally averaged flow, Q(x,t), and sea-surface elevation, H(x,t), in the model channel are:

Continuity: $$\frac{\partial H}{\partial t} - \frac{1}{b}\frac{\partial Q}{\partial x} = 0 \tag{6}$$

Momentum: $$\frac{\partial Q}{\partial t} + \frac{\partial}{\partial x}\left(\frac{Q^2}{A}\right) = -gA\frac{\partial H}{\partial x} - \frac{F}{A \cdot R}|Q|Q \tag{7}$$

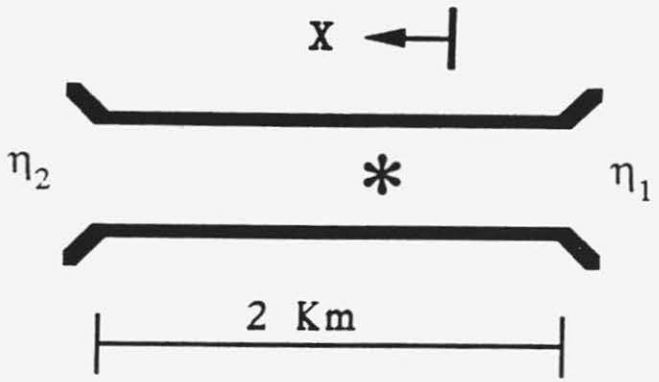

Figure 7. The hypothetical tidal channel for the model. The pond symbol marks the grid point at which tidal current and sea-surface are examined.

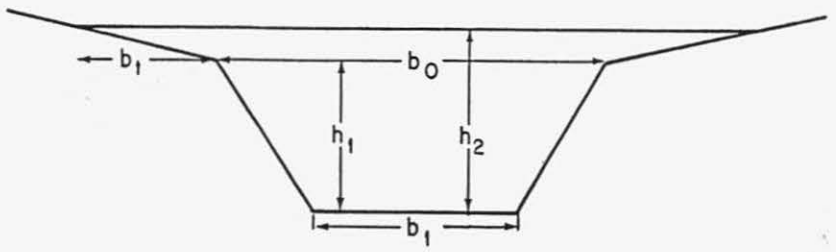

Figure 8. The geometry of the trapezoidal channel cross-section:
b_1 = 200 m, width of channel at its base
b_o = 350 m, width of channel at its tip
b_t = 400 m, width of tidal flat
h_1 = 1.85 m, channel depth
h_2 = undisturbed water depth

where b is the width, A is the cross-section, R is the hydraulic radius of the channel, and F=0.02, is a friction parameter. This formulation has been shown to be suitable for strongly non-linear systems (Speer and Aubrey, 1985; Aubrey and Friedrichs, 1988). The governing equations were solved numerically, using an explicit, leap-frog finite difference scheme. The model consists of 9 grid points with spacings of 250 m, and time-steps of 15 sec.

The boundary conditions are assumed as follows:

$$\text{at } x = 0, \quad \eta_1 = a_1 \cos(\varpi t)$$

$$\text{at } x = L, \quad \eta_2 = a_2 \cos(\varpi t - \phi)$$

where L is the length of the channel, a_1 and a_2 are tidal amplitudes at the two open ends of the channel, ϕ is the tidal phase difference, h_o is the mean sea-level difference, and ω is the M_2 tidal frequency. a_1 is fixed to be 1 m, and the still water depth at x=0 is set to 2.5 m. During the model exercises, the values of a_1/a_2, f, and h_o are varied one at a time. The tidal characteristics produced by each model run at the grid point corresponding to the current meter deployment in West Channel are examined, and their Lagrangian, Eulerian, and Stokes velocities and transports are calculated.

Model Results

Influence of the Tidal Amplitude Difference

The model was run for 7 cases in which a_1/a_2 was set to be 0.5, 0.75, 1.0, 1.25, 1.5, 2.0, and 2.5, respectively, while ϕ and h_o were set to zero. When the tidal amplitude at x=L is greater ($a_1/a_2 < 0$), the instantaneous tidal current speed and sea-surface elevation in the interior of the channel are in quadrature (Fig. 9a). The tidal current shows easterly dominance as indicated by the greater negative speed and sharper gradient around the time of maximum water elevation (Fig. 9a). As a result of this flow dominance, the Eulerian, Stokes, and Lagrangian residual currents and transport are directed towards the east (Figs. 9b,c).

When $a_1/a_2 = 1$, the sea-surface in the interior of the channel simply co-oscillates with the tides at the two ends, and there is little current in the channel (Fig. 9a). The result is no residual current or transport through the channel (Figs. 9b,c).

When a_1/a_2 becomes greater than unity, the instantaneous tidal current and sea-surface elevation in the interior of the channel are in phase. The flow shows a westward dominance. As a_1/a_2 increases, so does the amplitude of the instantaneous tidal flow and the asymmetry between the flood and ebb currents (Figs. 9a,c), a condition that results in the increase of westward residual velocities and transports (Figs. 9b, c).

The sensitivity analysis of residual current-generation to the tidal amplitude differences shows that the residual current curves become asymmetrical about unity (Fig. 9d). Since the value of a_1 is fixed at 1 m, as a_1/a_2 increases beyond unity, a_2 becomes smaller, which results in the asymptotically slow increase of residual velocities. On the other hand, when a_1/a_2 decreases below unity (a_2 greater than 1 m), the magnitude of residual currents increases quickly due to the approach of a_2 to the mean water depth (h=2.5 m), causing stronger non-linearity in the system. The boundary tidal amplitude differences do not affect the characteristics of the tide in the interior of the channel, except that the phasing between the instantaneous tidal current and sea-surface elevation varies between zero and 180 degrees depending on which end of the channel has greater tidal amplitude.

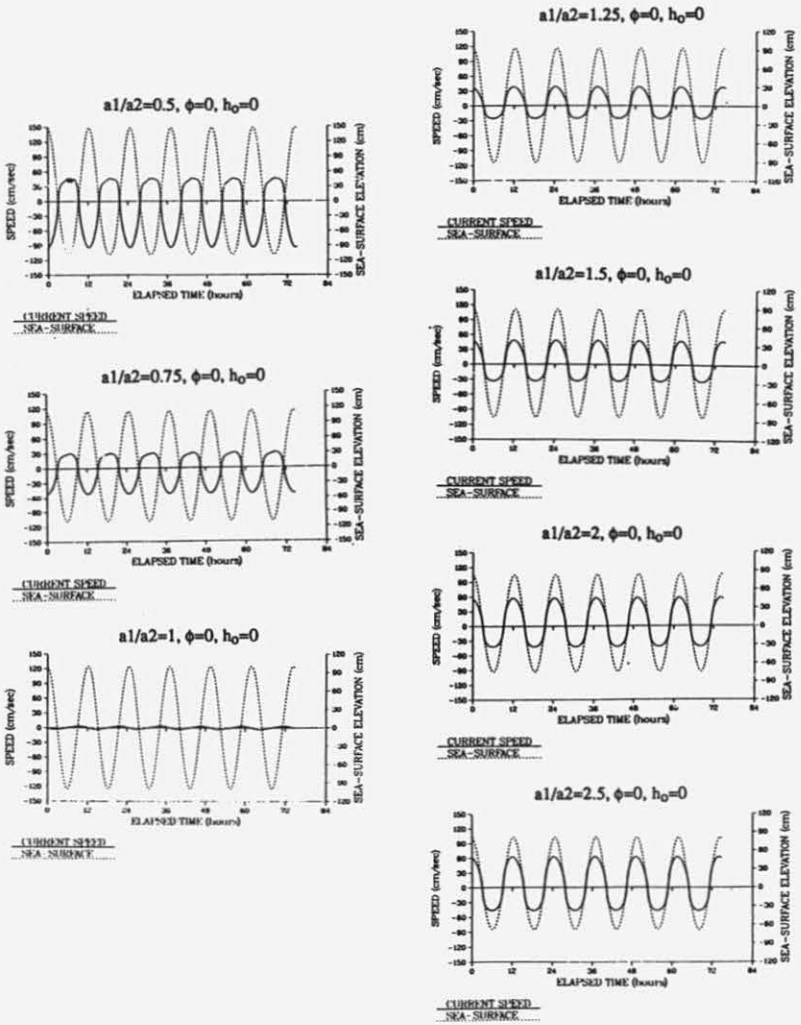

Figure 9. Influence of tidal amplitude differences:
(a) Instantaneous tidal current speed and sea-surface

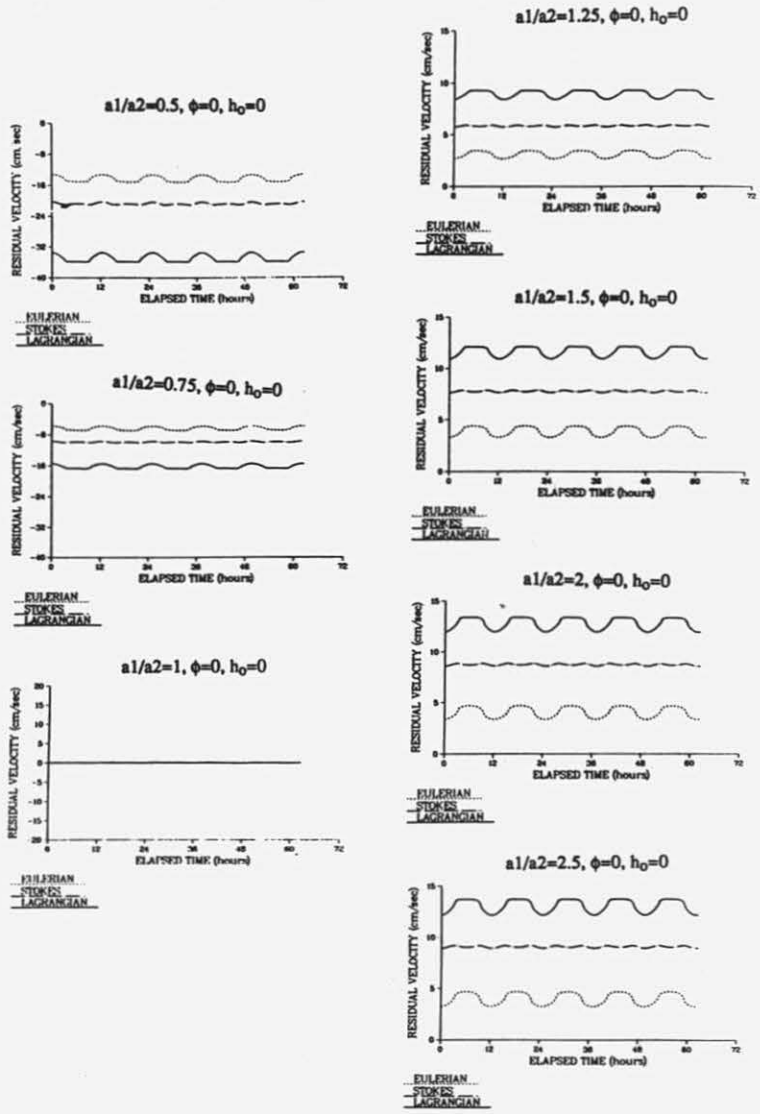

(b) Residual currents

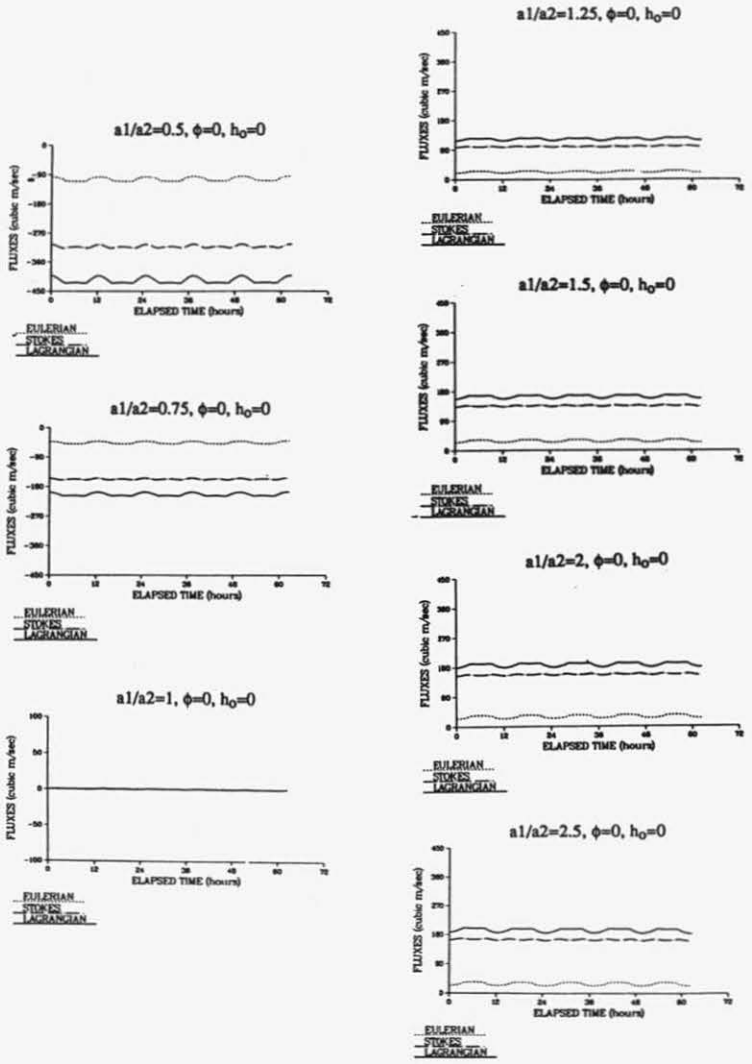

(c) Residual transports

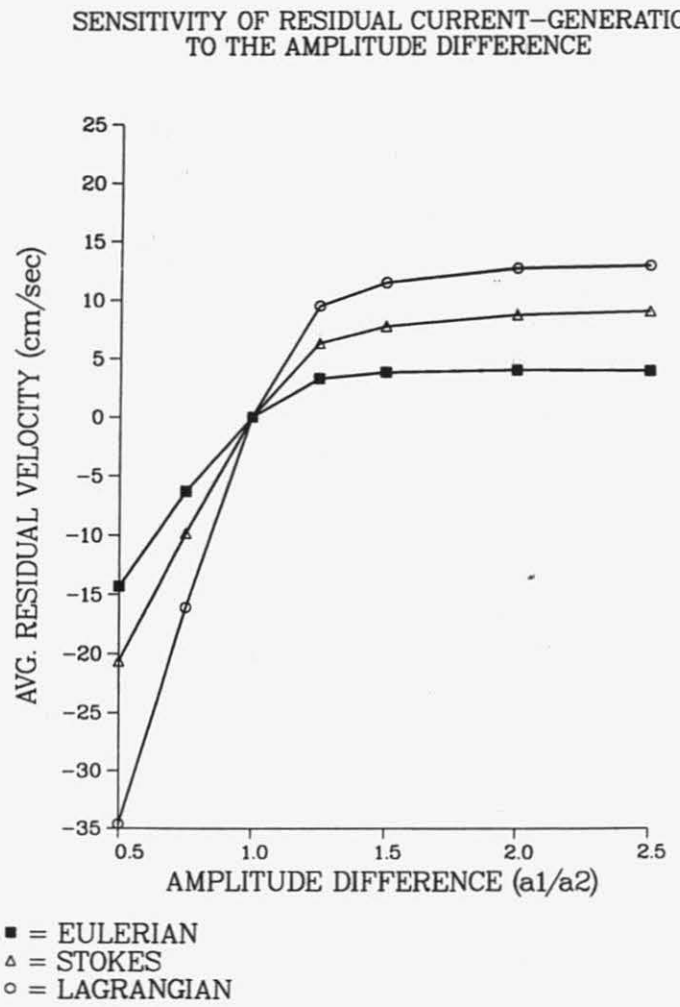

(d) Residual currents versus tidal amplitude differences

Influence of the Tidal Phase Difference

The influence of tidal phase difference was tested for ϕ = -90, -60, -30, 30, 60, and 90 degrees. In cases of negative phase differences when the phase at x=L leads that at x=0, the sea-surface elevation leads the instantaneous tidal flow in the interior of the channel (Fig. 10a). The Stokes drift is eastward, whereas the Eulerian and Lagrangian velocities are in the opposite direction (Fig. 10b). When ϕ is near -90 degrees, the Stokes transport dominates the opposing Eulerian transport, so that the resultant Lagrangian transport is in the direction of the Stokes transport (Fig. 10c). As ϕ tends towards zero, Eulerian transport becomes dominant, and the Lagrangian transport is in the direction of the Eulerian transport (Fig. 10c).

In cases of positive phase differences, the sea-surface lags behind the instantaneous tidal flow in the interior of the channel (Fig. 10a). The Stokes velocity remains positive (westwards) in all cases, but the Eulerian velocity changes direction from westward to eastward as ϕ increases towards 90 degrees (Figs. 10b,c). The Stokes transport dominates when ϕ is positive, so that the resultant Lagrangian transport is in the same direction as the Stokes transport (Fig. 10c).

The tidal phase difference appears not to change the direction of the Stokes velocity, which remains westwards in all cases. For negative ϕ's, the Eulerian flow is constantly easterly (negative). But for positive ϕ's, the direction of the Eulerian flow is variable (Fig. 10d).

Influence of the Mean Sea-level Difference

The influence of the mean sea-level difference was tested for h_o = -0.1, -0.05, -0.01, 0.01, 0.05, and 0.1 m. A mean sea-level difference creates a noticeable mean flow (Fig. 11a). In addition, the amplitude of the tidal flow is suppressed.

Physically the change of h_o is analogous to tilting the sea-level along the channel, having the pivotal point at x=0. Negative h_o creates a westward sloping sea-surface, thereby resulting in westerly residual currents (Figs. 11a,

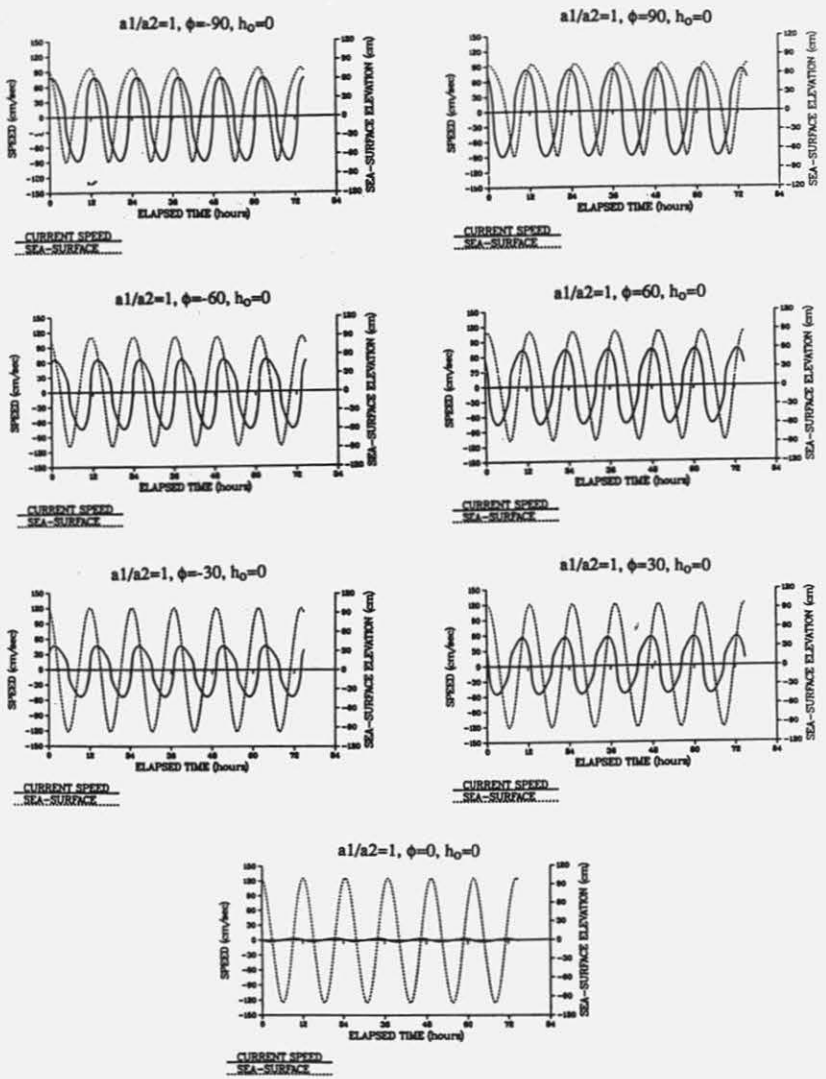

Figure 10. Influence of tidal phase differences:
(a) Instantaneous tidal current speed and sea-surface

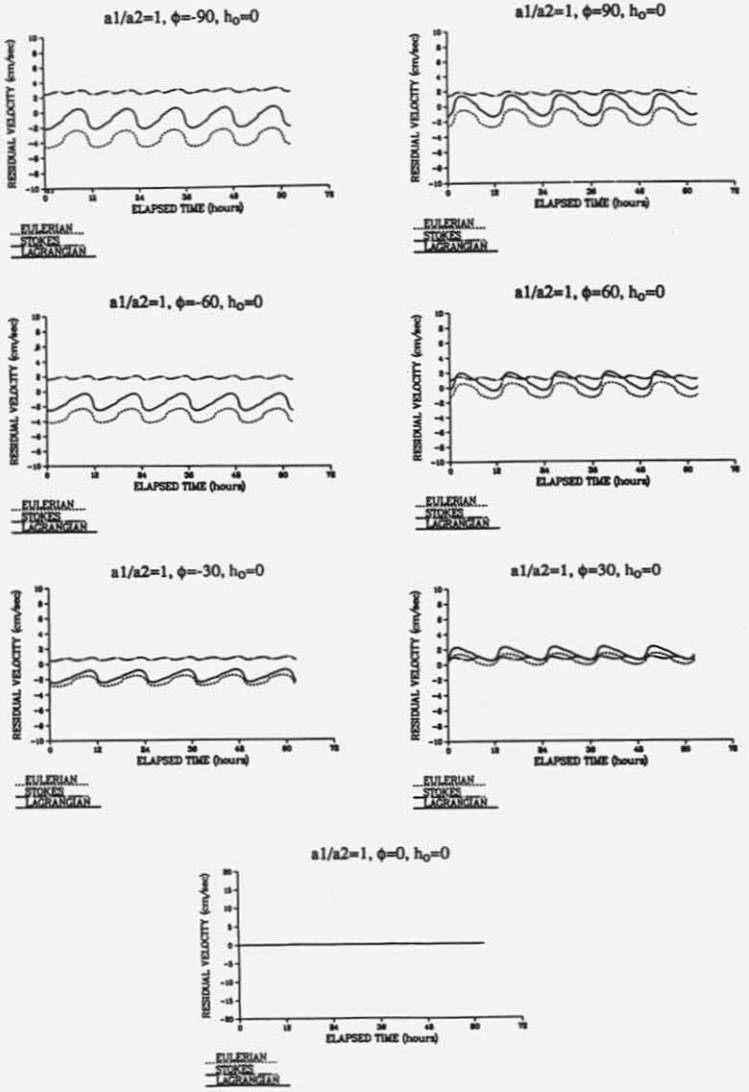

(b) Residual currents

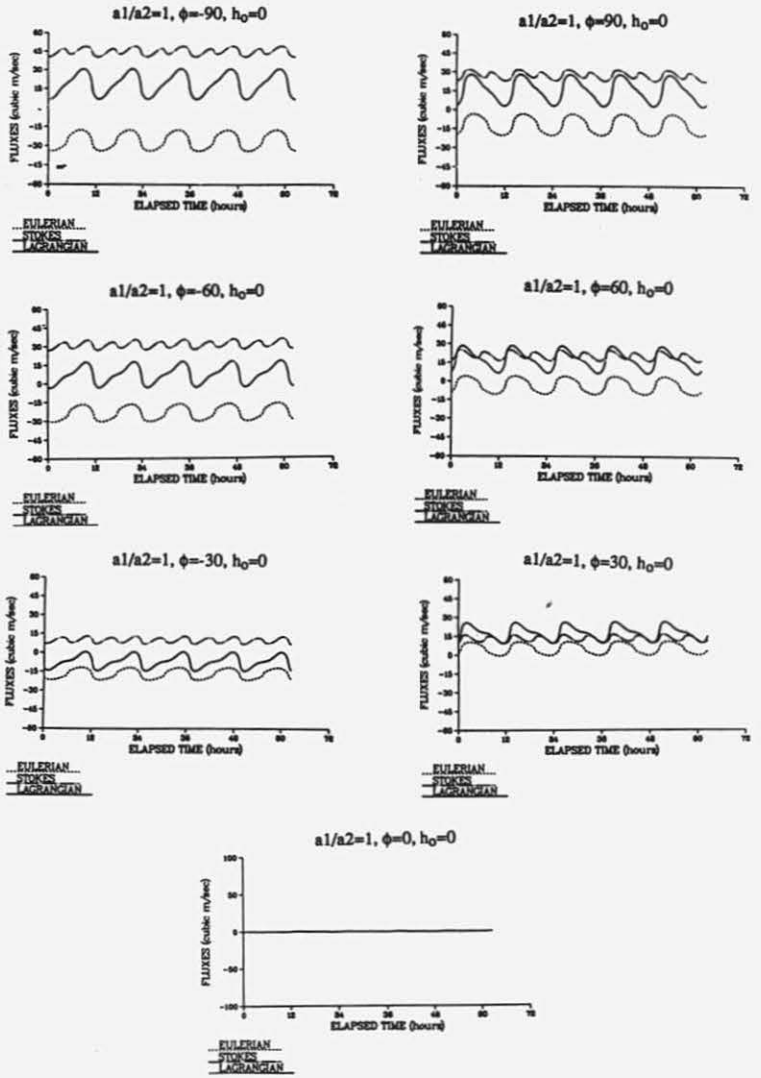

(c) Residual transports

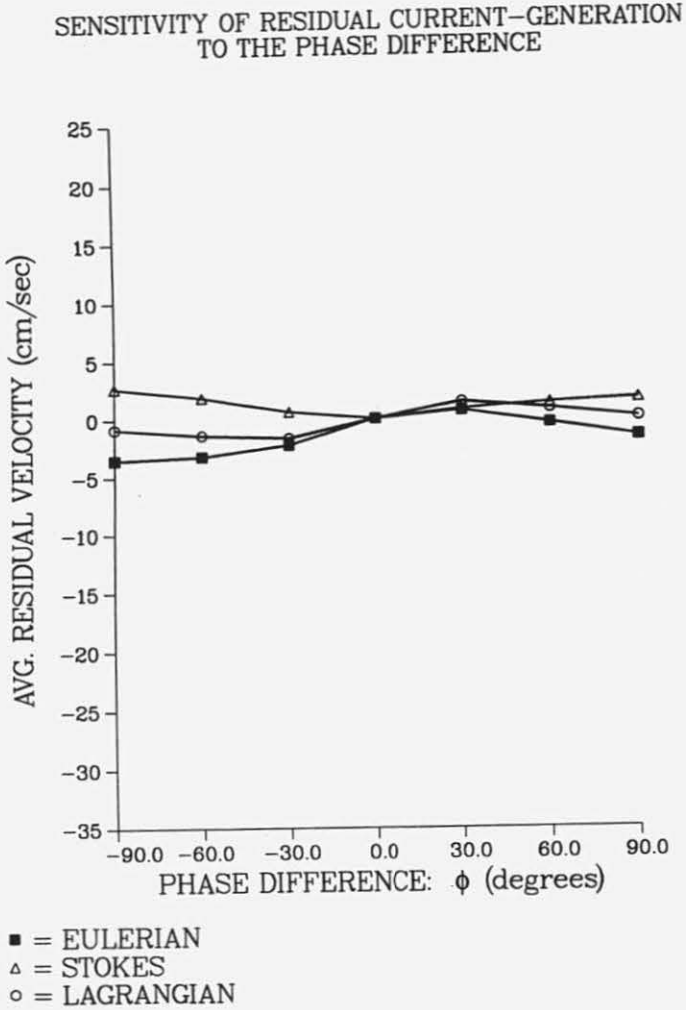

(d) Residual currents versus tidal phase differences

b). On the other hand, a positive h_o results in easterly flows. Within the suppressed instantaneous tidal flow in the interior of the channel, there is a tidal asymmetry in the presence of a residual flow (Fig. 11a). However, as the absolute value of h_o increases, this tidal asymmetry in the instantaneous flow gradually disappears. In general, for corresponding h_o of opposite signs, the residual velocities and their transports are identical in magnitude, but are rotated 180 degrees and symmetrical around the 0-axis (Figs. 11a, b, c).

In the case of mean sea-level difference, the Stokes velocity and transport are fairly insignificant, compared to the Eulerian velocity and transport (Figs. 11c, d). Due to the shortness of the channel (2 km long), the system is sensitive to the difference in the mean sea-level. Numerical model results indicate that even a slight h_o of 1 cm in either direction can produce a pressure gradient on the order of 10^{-5}, which can result in residual Eulerian flows of 5 cm/sec.

Discussion

The Generation of M_4 Overtide

The generation of residual currents in a tidal channel is most sensitive to the mean sea-level difference (Fig. 11d), less sensitive to the tidal amplitude difference (Fig. 9d), and least sensitive to the tidal phase difference (Fig. 10d) between the two ends. One the other hand, the Eulerian residual currents produced by the tidal phase differences show distinctive modulations at semi-diurnal frequencies (Fig. 10b). Eulerian residual currents produced by tidal amplitude differences show slight semi-diurnal modulations (Fig. 9b), and those produced by the mean sea-level differences have little modulation (Fig. 11b). These modulations might have been introduced by the time-averaging process to obtain residuals, and therefore, probably do not reflect the physics. In order to understand the discrepancies among the characteristics of the instantaneous and residual currents generated by different boundary conditions, it is worthwhile to investigate the generation of the M_4 overtide (the first harmonic of M_2) in the interior of the channel associated with the changing boundary conditions, since both the M_4 overtide and residual currents are related to the non-linearity in the system (Pingree and Maddock, 1977; Prandle, 1978).

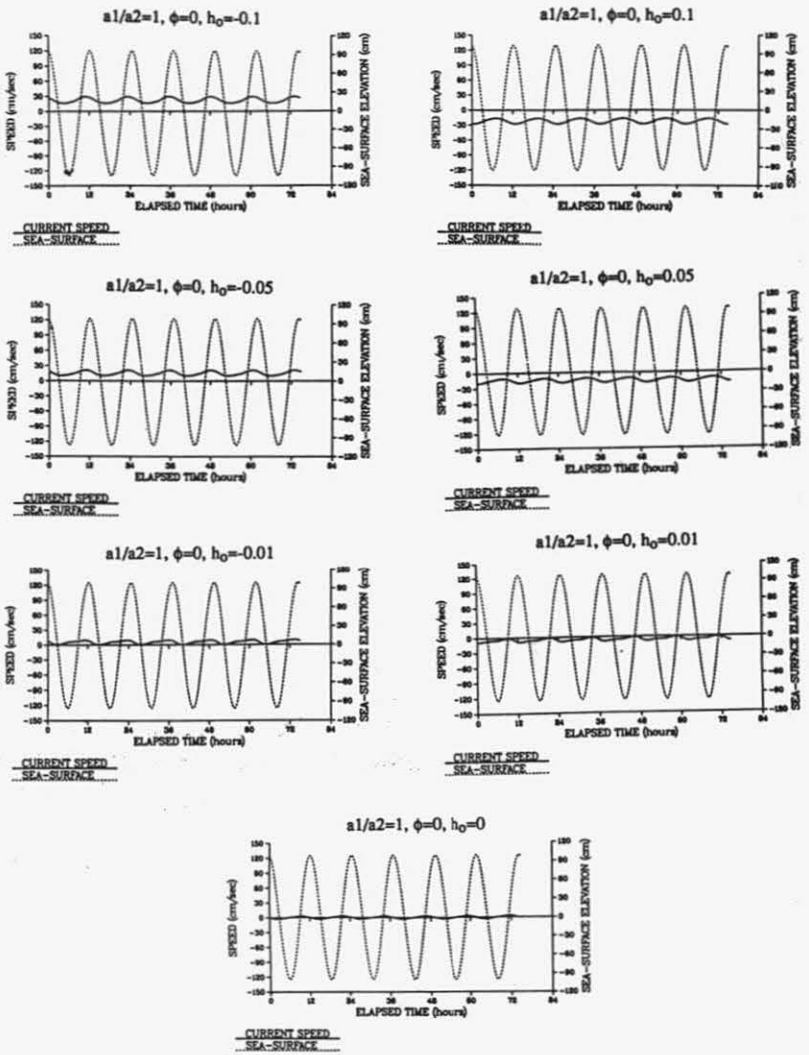

Figure 11. Influence of mean sea-level differences:
(a) Instantaneous tidal current speed and sea-surface

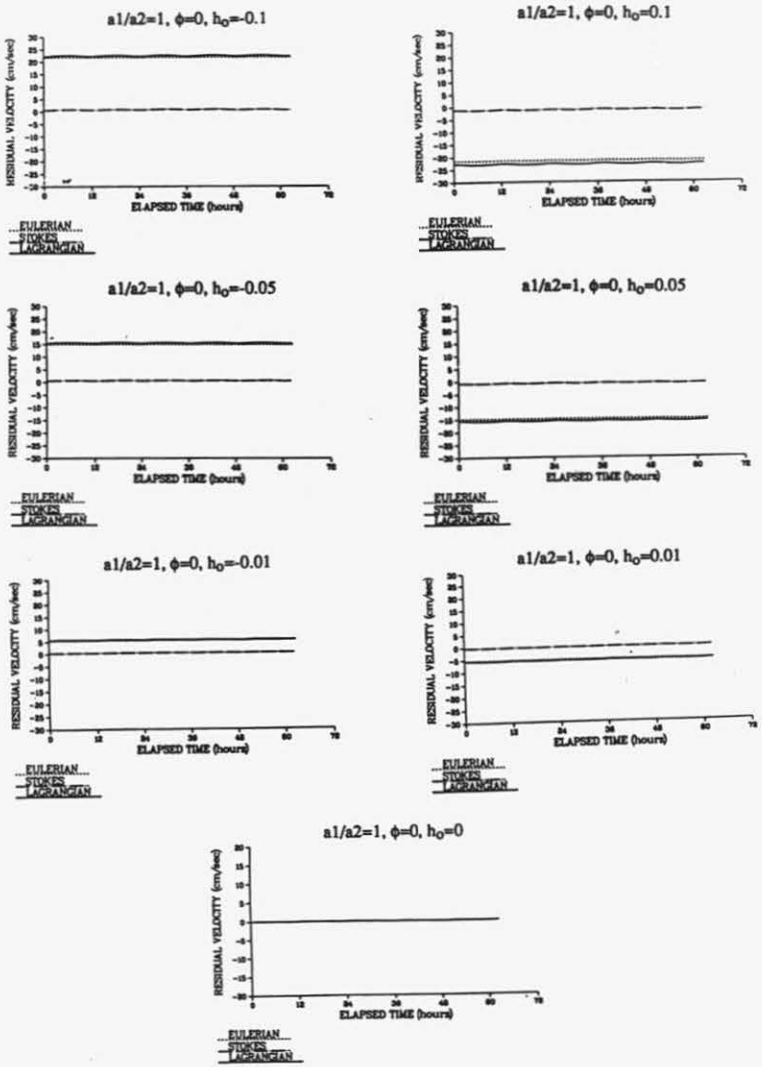

(b) Residual currents

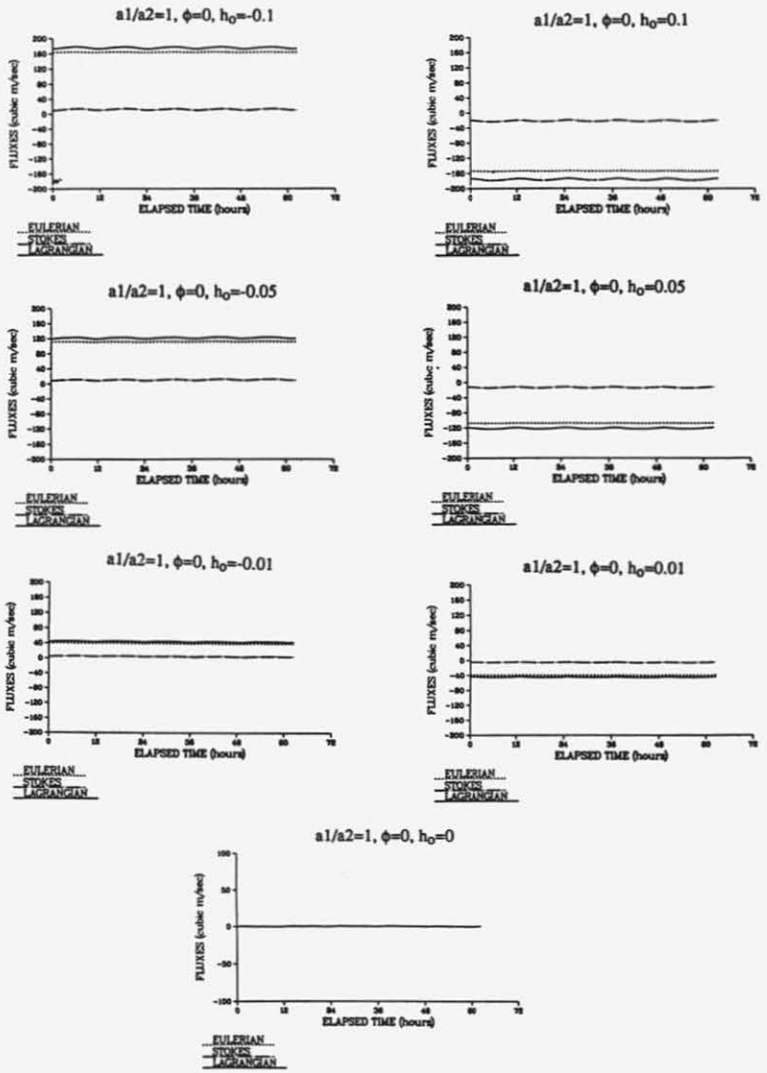

(c) Residual transports

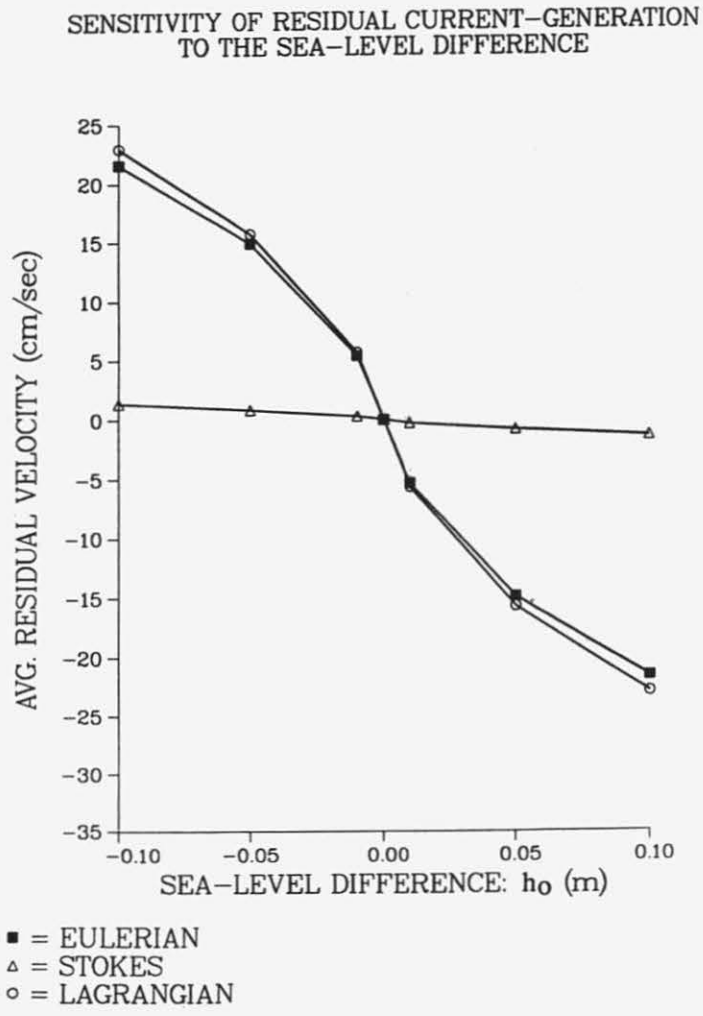

(d) Residual currents versus mean sea-level differences

The M_4/M_2 ratio, which is an indication of non-linearity, and the M_4 relative phase are plotted against the model variables (Figs. 12a, b, and c). The M_4 relative phase is defined as $\theta_{M4} = 2\,\phi_{M2} - \phi_{M4}$, where ϕ_{M2} and ϕ_{M4} are M_2 and M_4 phases respectively. M_4/M_2 is most sensitive to the tidal phase differences, less sensitive to the tidal amplitude differences, and least sensitive to the mean sea-level differences. Sea-level differences tend to suppress the generation of overtides, and the tidal amplitude differences have intermediate influence on the generation of overtides. The tidal amplitude differences have moderate effects on the non-linearity of the instantaneous and residual currents.

Friction Effects on Model Results

The distinctions between residual current and M_4 generation suggest different mechanisms to generate residual currents and overtides. Since in this particular system, the quadratic friction is the dominant non-linear term, it is helpful to examine it closely. Heath (1980) expressed the quadratic friction in his depth-integrated equation as:

$$\frac{r}{h+\zeta}\,|u_1 + u_2 + u_0|\,(u_1 + u_2 + u_0) \qquad (8)$$

where r is the quadratic friction coefficient, h is the undisturbed water depth, z is the sea-surface elevation, u_1 and u_2 are M_2 and M_4 speeds respectively, and u_0 is the residual current. Through expansion of eq. 8, Heath identified four major terms in the friction as the production of M_2 tidal energy, the input to M_4 tide, the frictional dissipation of M_4, and the input to the mean flow. Although Heath (1980) did not address the issue of the generation of M_4 and residual currents, his analysis does give a clear picture of different frictional contributions to the M_4 overtide and the residual flow. When mean sea-level differences exist, the residual flow generation overwhelms the harmonic generation, and *vice versa* in the case of tidal phase differences. At this point, the physics of the M_4 generation, its relative phase, and residual currents are not clear.

To examine further the friction effects on model results, two additional values of 0.1 and 0.005 were used for the friction parameter in the model. Curves of M_4/M_2 and M_4 relative phase versus model variables having different friction parameters show that they are identical, except for some variation in the M_4

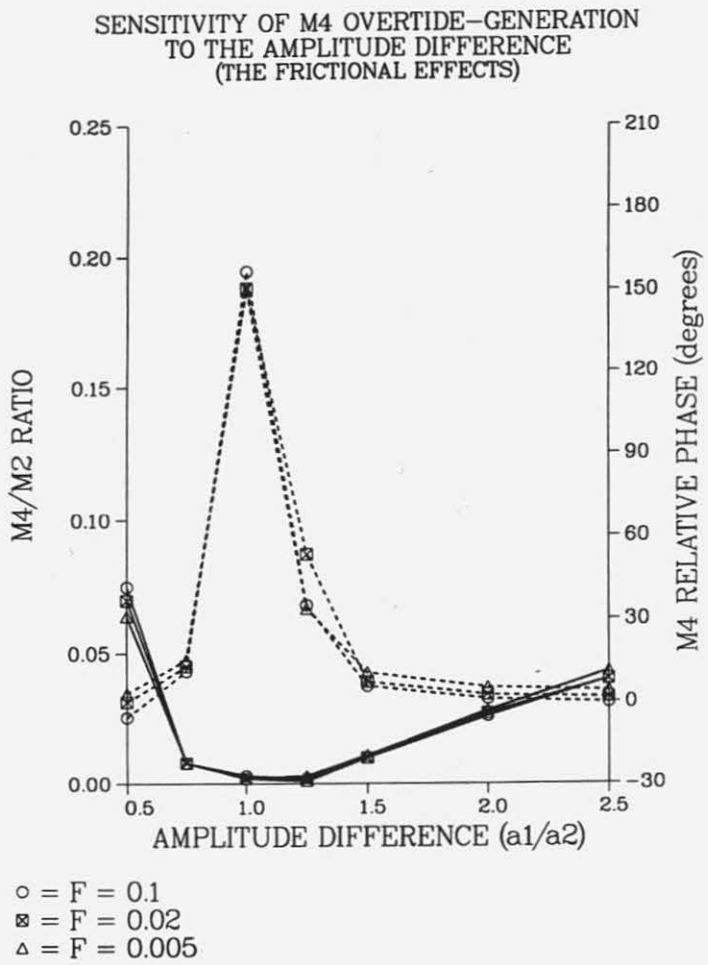

Figure 12. M_4/M_2 (solid lines) and M_4 relative phase (dashed lines) versus: (a) Tidal amplitude differences

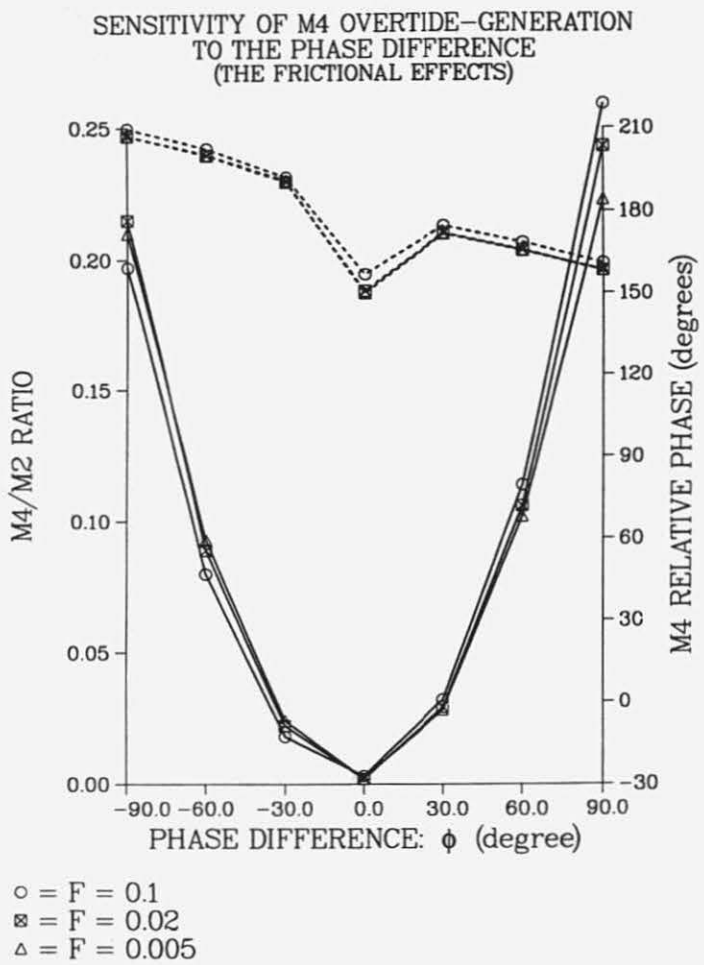

(b) Tidal phase differences

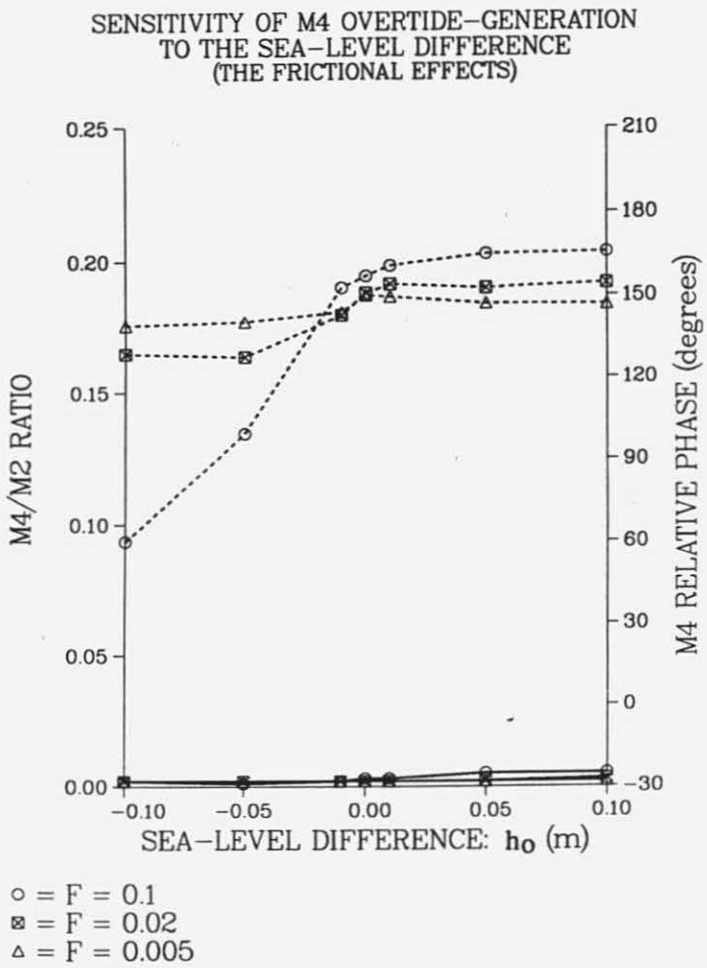

(c) Mean sea-level differences with 3 different friction parameters

relative phase in the case of mean sea-level differences (Figs. 12a, b and c). The resemblance among these curves indicate that the generation of M_4 overtides is little affected by the friction. In other words, overtides are most likely to be related to the kinematic non-linearity that entered through continuity, which means the geometry of the channel plays an important role in introducing overtides to the system.

On the other hand, higher friction in the system does reduce the magnitude of Lagrangian residual currents and *vice versa* (Figs. 13a, b and c). The friction effect is greatest in the case of mean sea-level differences (Fig. 13c), intermediate in the case of amplitude differences (Fig. 13a), and the smallest in the case of phase differences (Fig. 13b). The different sensitivity of the generation of residual currents and overtides to the friction further indicates that different mechanisms are responsible for the generation of the two in a non-linear system.

Comparisons of Model Results with Field Data

Harmonic analysis of the tidal records from south Chatham Harbor and Nantucket Sound indicates that $a_1/a_2 = 1.7$ and the phase difference is ϕ=5.5 degrees for the M_2 tide between the two ends of West Channel (Tables 1 and 2). The diagnostic model indicates a tidal amplitude difference of $a_1/a_2 = 1.7$ only can produce a westerly Eulerian residual current of approximately 5 cm/sec. The contribution from the tidal phase difference of $\phi = 5.5$ degrees is almost undetectable. In order to produce a model residual current having a magnitude comparable to that is observed in the field, a mean sea-level difference between south Chatham Harbor and Nantucket Sound is needed; this pressure gradient has to be from south Chatham Harbor down towards Nantucket Sound. Subsequently, trial model runs were conducted, using $a_1/a_2 = 1.7$, $\phi = 5.5°$, and varying h_o ($h_o < 0$). The value $h_o = -15$ cm generates an instantaneous tidal current that approximates the observed flow, where the maximum westward current magnitude is approximately twice that of the eastward flow (Figs. 14, 5). This finding suggests that the mean sea-level in south Chatham Harbor may be roughly 15 cm higher than that of Nantucket Sound. However, our field observations were not accurate enough to verify this difference in mean water levels.

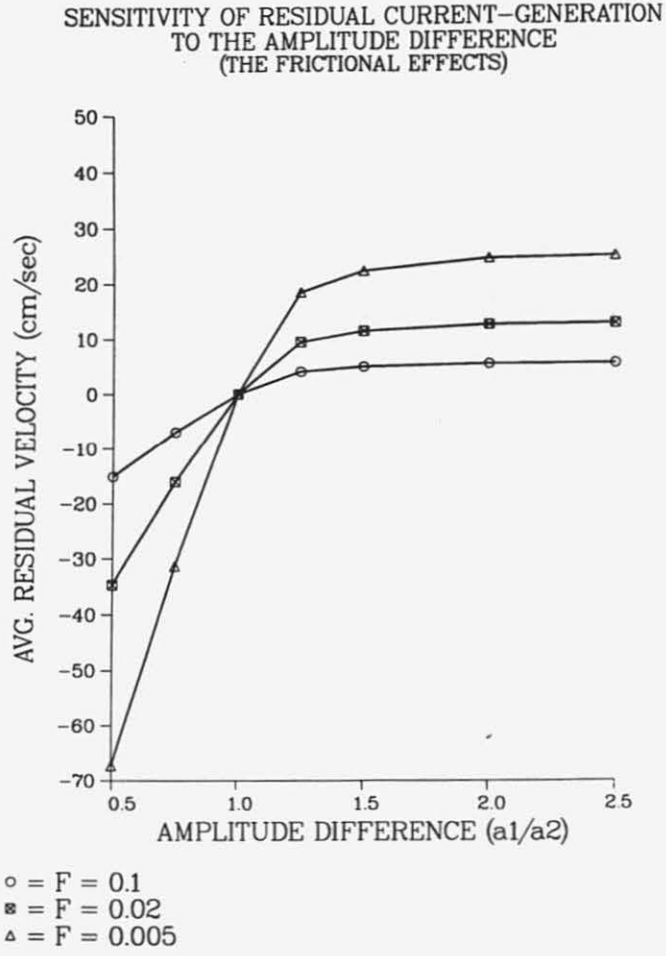

Figure 13. Friction effects on the generation of residual currents in cases of (a) Tidal amplitude differences

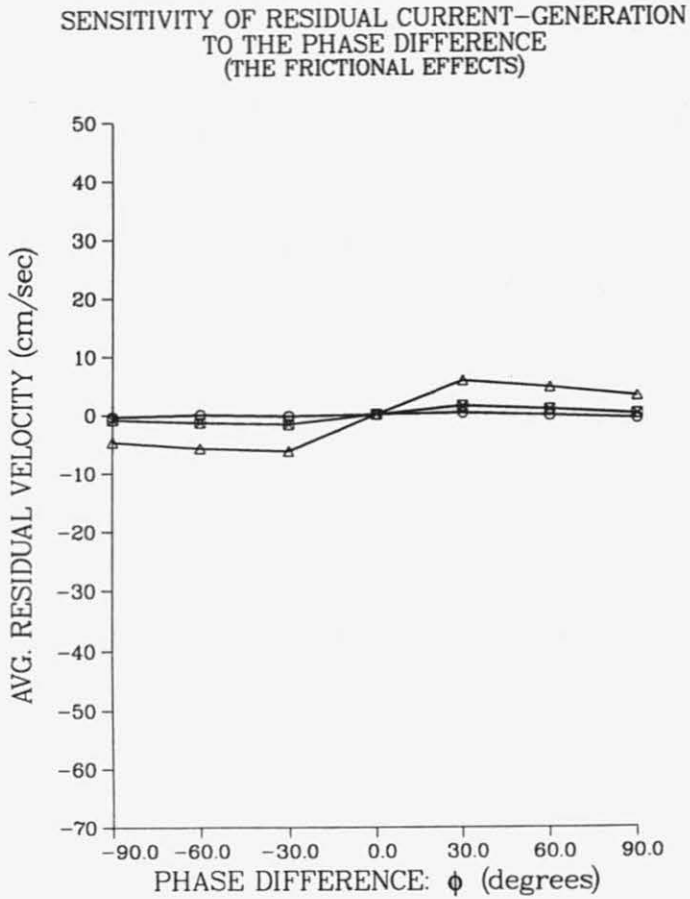

(b) Tidal phase differences

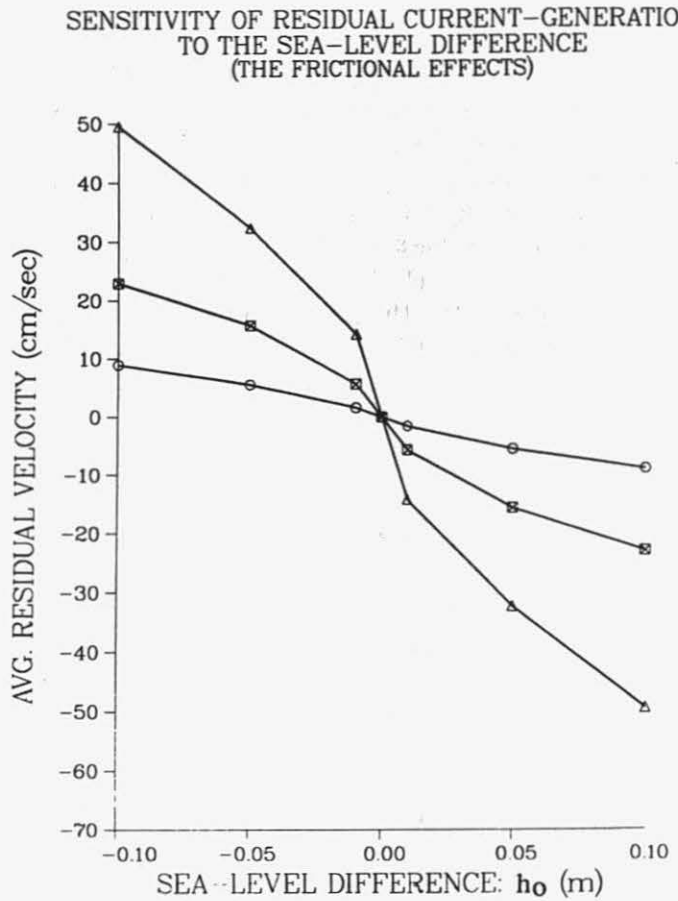

(c) Mean sea-level differences

Since the tidal currents were measured at a point, and the model simulation produces sectionally averaged flows, no direct comparison can be made between the two without invoking some additional constraints. In order to compare the field observation and the model simulations, sectionally averaged 'field data' were generated by applying the measured sea-surface in south Chatham Harbor and Nantucket Sound and a mean sea-level difference of -15 cm. The spectral results more closely approximate the field data (Fig. 15). The residual currents from the 'real-time' model show fluctuations at tidal and subtidal frequencies (Fig. 15). The tidal frequencies indicate incomplete filtering in our analysis, whereas the subtidal frequencies may represent nonlinear physics. The mean value for the Lagrangian transport of the 'real-time' model (Fig. 15) is approximately the same as that of the line spectral (single frequency) model (Fig. 14). Therefore, that the mean sea-level in south Chatham Harbor is approximately 15 cm higher than that in Nantucket Sound appears consistent.

Model Comparison

To understand further the combined effects of tidal amplitude, phase, and mean sea-level differences on the generation of residual currents, the numerical model was modified to have a rectangular channel; these results were compared with an analytical model developed by van de Kreeke (1980), having linearized friction and rectangular channel cross-section. The solution of van de Kreeke's model for tidally-averaged flow, $\bar{q}$, in the middle of the channel is expressed as:

$$\frac{\bar{q}T}{hL} = P\frac{a_1 a_2}{h^2}\sin(\phi) + Q\frac{a_1^2 - a_2^2}{h^2} + \frac{C_o h}{F_1 L}\frac{\lambda}{L}\frac{h_o}{h} \qquad (9)$$

in which h is the undisturbed water depth, T is the M_2 period, L is half the channel length, λ is the tidal wave length for zero friction, $C_o = \lambda/T$, F_1 is the linearized friction, and P and Q are functions of $(C_o h) / (F_1 L)$ and λ/T. The values for P and Q were extrapolated from tables in van de Kreeke and Dean (1975) to be 75 and 12, respectively. The three terms on the right hand side of eq. 9 are the contributions from the tidal phase, amplitude, and mean sea-

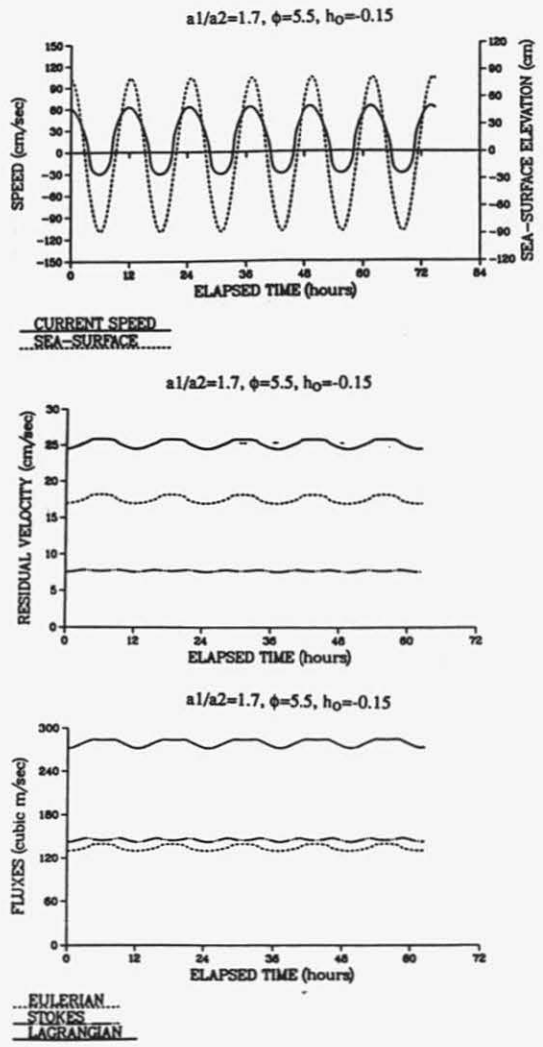

Figure 14. Theoretical simulation of instantaneous tidal currents, sea-surface, residual currents, and residual transports in West Channel.

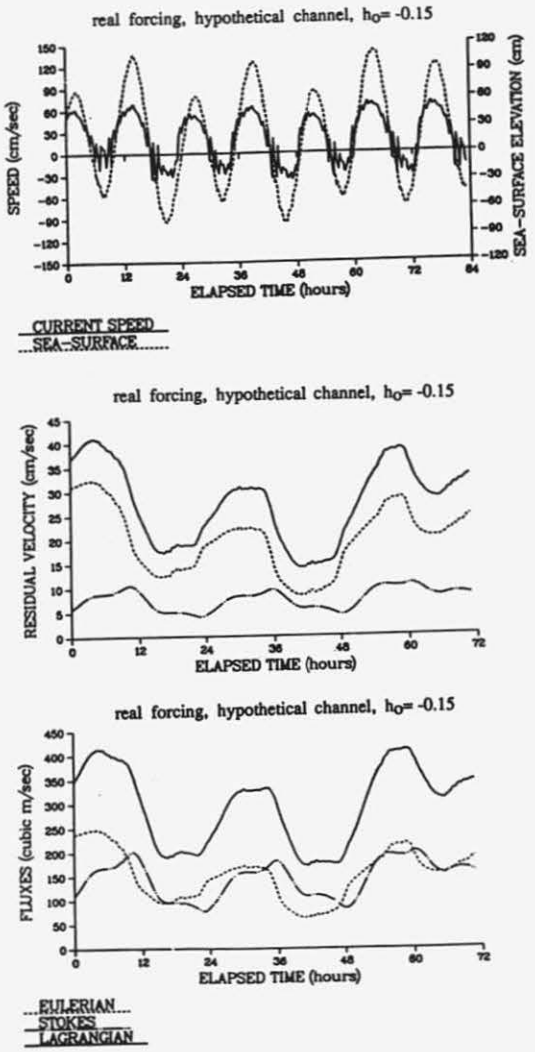

Figure 15. Simulation of instantaneous tidal currents, sea-surface, residual currents, and residual transports by applying the 'real-time' forcings and h_o = -0.15 m through the model channel.

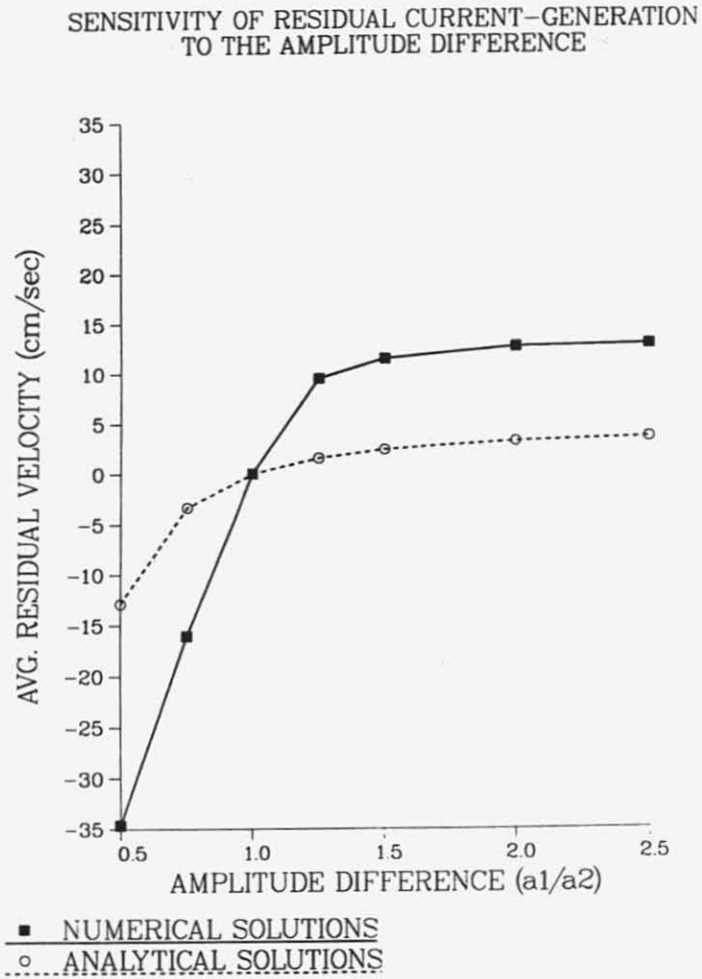

Figure 16. Model comparisons in cases of:
(a) Tidal amplitude difference

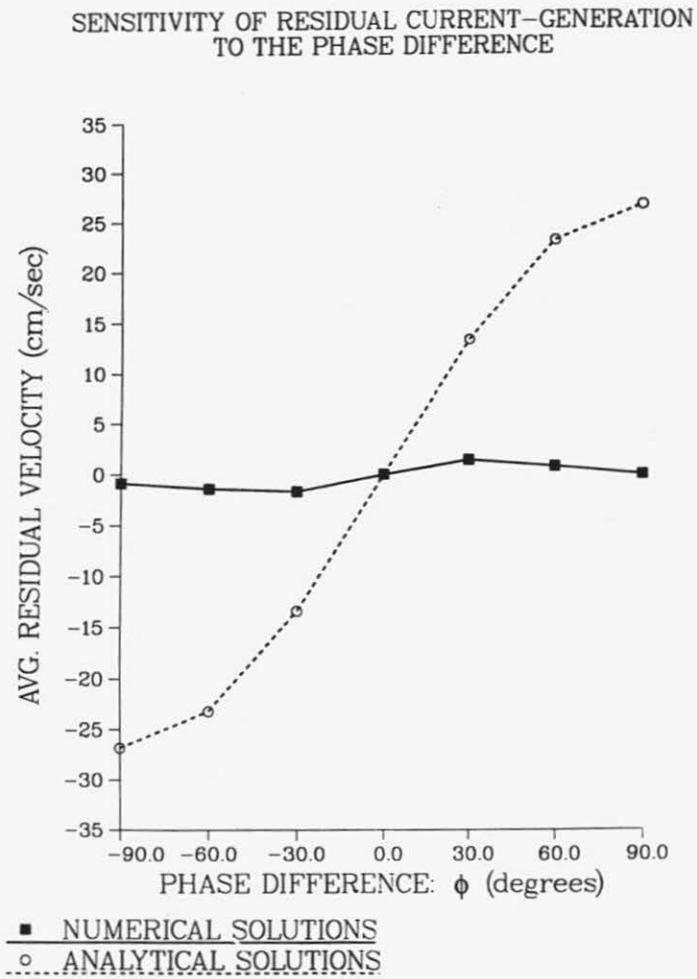

(b) Tidal phase difference

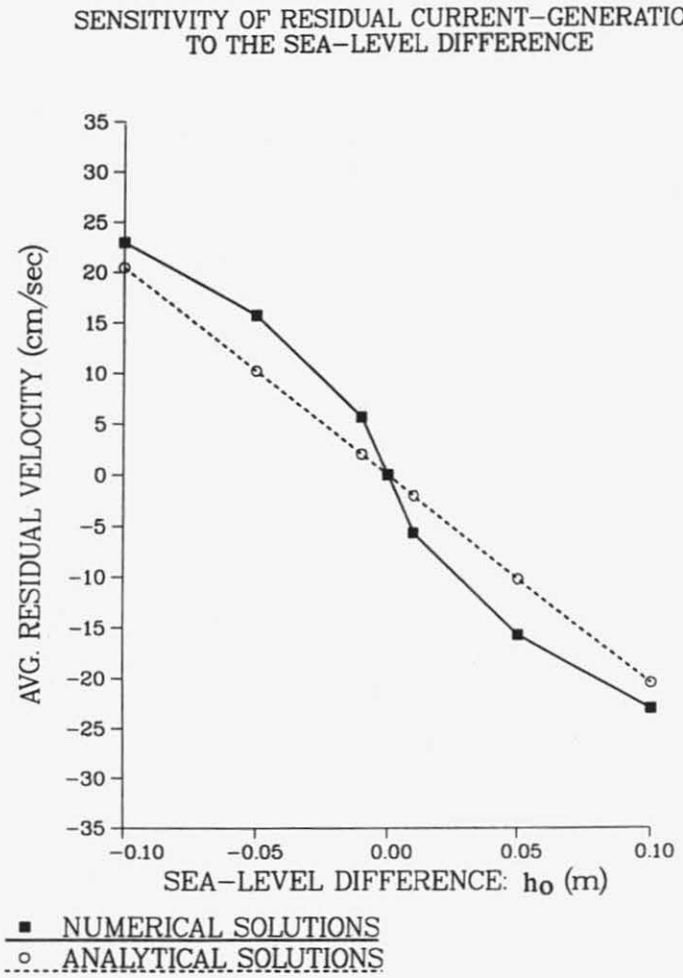

(c) Mean sea-level difference

level differences to the residual currents in the channel, respectively. Equation 9 also suggests that these contributions are linear. The two models agree well in the case of mean sea-level differences (Fig. 16c), they agree marginally in the case of amplitude differences (Fig. 16a), and they disagree significantly in the case of tidal phase differences (Fig. 16b). The disagreement reflects the inadequate consideration of non-linear effects by the analytical solution, which effects have been shown by our model to be important. For parameters that characterize the residual currents in West Channel, (a_1/a_2 = 1.7, ϕ = the tidal phase, amplitude, and mean sea-level differences are proportional to 1: 2 : 20. The analytical model concurs with the numerical model findings that the mean sea-level difference is the most influential factor in the generation of residual currents. However, the magnitude of the residual currents predicted by the analytical model is 35 cm/sec, compared to 18 cm/sec predicted by the numerical model. The higher value from the analytical model is probably due to the unrealistic linear expression of the three contributions in the solution. For instance, the numerical result of the Eulerian residual current for $a_1/a_2 = 1.7$, ϕ and $h_o = 0$, is 5 cm/sec; for $a_1/a_2 = 1$, $\phi = 0$, and $h_o = -0.1$, is 22 cm/sec. But for $a_1/a_2 = 1.7$, $\phi = 5.5°$, and $h_o = -0.15$, the residual current speed is only 18 cm/sec. Clearly the numerical results do not simply add up as the analytical solution suggests. Therefore, the influence of the tidal amplitude, phase, and mean sea-level differences on the generation of residual currents is interactive and non-linear, and can only be expressed clearly by nonlinear numerical modeling.

Conclusions

a) The generation of residual currents in an open tidal channel is most sensitive to the mean sea-level differences, less sensitive to the tidal amplitude differences, and least sensitive to the tidal phase differences between the two ends of the channel.

b) The tidal phase difference between the two open boundaries of a channel is the most conducive to generating the M_4 overtide. The tidal amplitude differences have intermediate effect on the generation of M_4, and the mean sea-level differences have little effect on M_4 generation.

c) The field data depicting currents in West Channel can be fitted best by the model results for $a_1/a_2 = 1.7$ and a phase difference of $f = 5.5°$ for M_2 tide, and a mean sea-level difference of $h_o = -0.15$ m between south Chatham Harbor and Nantucket Sound. Sea-level in south Chatham Harbor is 15 cm higher than that in Nantucket Sound.

d) The residual current and M_4 overtide are generated by different mechanisms. The former is related more strongly to the friction within the system, and the latter is related more closely to the kinematic non-linearity in the system.

e) The combined influence of the tidal amplitude, phase, and mean sea-level differences between the two ends on the generation of residual currents in a tidal channel is interactive and non-linear, and can only be described properly by non-linear numerical models.

f) The historical evidence on the dominant westward sediment transport pattern observed in West Channel and the Monomoy breach suggests the existence of a mean current flowing from the Atlantic Ocean into Nantucket Sound. Field observation of tidal currents in West Channel indicates a strong westward residual current, having an average speed of 26 cm/sec. The tidal characteristics and residual flow in West Channel can be attributed best to the tidal amplitude and phase differences of the M_2 tides, but primarily a mean sea-level difference of 15 cm, between south Chatham Harbor and Nantucket Sound. Although the value of 15 cm may only apply to the 7-day period of the synoptic measurements of tidal heights and currents around West Channel, morphological data suggest that this difference may persist. Field data are inadequate to resolve this issue.

Acknowledgments

This study was partially funded by the Town of Chatham, the Commonwealth of Massachusetts through the Department of Environmental Management, the Coastal Engineering Research Center of the U.S. Army Corps of Engineers, the Coastal Research Center of Woods Hole Oceanographic Institution (WHOI), and NOAA National Sea Grant No. NA86-AA-D-SG090, WHOI

Sea Grant Project No. R/O-6. The U.S. Government is authorized to produce and distribute reprints for governmental purposes notwithstanding any copyright notation that may appear hereon. We thank Drs. Richard Signell and Wayne R. Geyer for reviewing an early version of the manuscript. Woods Hole Oceanographic Institution Contribution No. 8318.

References

Aubrey, D.G. and C.T. Friedrichs, 1988. Seasonal climatology of tidal non-linearities in a shallow estuary. In: *Hydrodynamics and Sediment Dynamics of Tidal Inlets*, Aubrey, D.G. and L.Weishar (eds.), Springer-Verlag, NY, p. 103-124.

Cotter, D.C., 1974. Tide-Induced Net Discharge in Lagoon-Inlet Systems. Master's thesis, University of Miami, 40 pp.

Giese, G.S., 1988. Cyclical behavior of the tidal inlet at Nauset Beach, Chatham, Massachusetts. In: *Hydrodynamics and Sediment Dynamics of Tidal Inlets*, Aubrey, D.G. and L. Weishar (eds.), Springer-Verlag, NY, p. 269-283.

Heath, R.A., 1980. Phase relations between the over- and fundamental-tides. *Dt. hydrogr. Z.*, v. 33 H (5), p. 177-191.

Hine, A.C., 1975. Bedform distribution and migration patterns on tidal deltas in the Chatham Harbor Estuary. In: *Estuarine Research*, v. 2, Cronin, L.E. (ed.), Academic Press, Inc., NY, p. 235-307.

Huang, P.-S., D.-P. Wang, and T.O. Najarian, 1986. Analysis of residual currents using a two-dimensional model. In: *Physics of Shallow Estuaries and Bays*, van de Kreeke (ed.), Springer-Verlag, NY, p. 71-80.

Ianniello, J.P., 1977. Tidally induced residual currents in estuaries of constant breadth and depth. *J. Mar. Res.*, v. 35, p. 755-786.

Ianniello, J.P., 1979. Tidally induced residual currents in estuaries of variable breadth and depth. *J. Phys. Ocean.*, v. 9, p. 962-974.

Liu, J.T., D.K. Stauble, G.S. Giese, and D.G. Aubrey, this volume. Morphodynamic evolution of a newly formed tidal inlet. In: Aubrey, D.G. and G.S. Giese, (eds.), *Formation and Evolution of Multiple Inlet Systems, Coastal and Estuarine Studies Series*, AGU.

Pingree, R.D. and L. Maddock, 1977. Tidal residuals in the English Channel. *J. Mar. Biol. Ass. U.K.*, v. 57 (2), p. 339-354.

Prandle, D., 1978. Residual flows and elevations in the southern North Sea. *Proc. R. Soc. Lond. A.*, v. 359, p. 189-228.

Speer, P.E., and D.G. Aubrey, 1985. A study of non-linear tidal propagation in a shallow estuarine system, part 2: theory. *Estuarine, Coastal and Shelf Sci.*, v. 21, p. 207-224.

Tee, K.T., 1976. Tide-induced residual current, a 2-D non-linear numerical model. *J. Mar. Res.*, v. 34, p. 603-628.

Tee, K.T., 1977. Tide-induced residual current-verification of a numerical model. *J. Phys. Oceanogr.*, v. 7, p. 396-402.

van de Kreeke, J., 1978. Mass transport in a coastal channel, Marco River, Florida. *Estuarine, and Coastal Mar. Sci.*, v. 7, p. 203-214.

van de Kreeke, J., 1980. Tide-induced residual flow. In: *Mathematical Modeling of Estuarine Physics*, Sundermann, J. and K.-P. Holz, (eds.), Springer-Verlag, NY, p.133-144.

van de Kreeke, J. and R.G. Dean, 1975. Tide-induced mass transport in lagoons. *J. Waterways, Harbor and Coastal Eng. Div.*, v, 4, p. 393-403.

Wong, K.-C., 1989. Tidally generated residual currents in a sea-level canal or tidal strait with constant breadth and depth. *J. Geophys. Res.*, v. 94, no. 6, p. 8179-8192.